Hydrogen-induced Sticker Breakouts in Continuous Casting of Steel: Chemical Reactions between Ambient Atmosphere, Molten Flux, Molten Steel and Solidified Shell

Yoshiyuki UESHIMA, Toshiaki MIZOGUCHI and Toshiyuki KAJITANI

Nippon Steel Corporation, Technical Development Bureau,

Shintomi 20-1, Futtsu, Chiba, 293-8511 Japan

Abstract: Hydrogen-induced sticker breakouts in aluminum-killed steel production without a degassing route have often been reported elsewhere, but so far, yet the mechanism has not been thoroughly explained quantitatively. In order to better understand this phenomenon, we analyzed hydrogen gas evolution from the solidified shell at the early stage of solidification. Moreover, new knowledge has been added for silicon-killed steel production with a degassing route by one of the present authors. Based on analyses, effective measures for stable casting have been carried out and such hydrogen-induced sticker breakouts have been successfully prevented.

Key-words: Hydrogen, Breakout, Continuous casting, Moisture, Mold powder, Solidified shell, NMR

1. Introduction

Prevention of caster breakouts is one of the most important issues when casting. One of the factors causing breakouts is hydrogen, as shown in Table 1.

Table 1 Frequency of hydrogen-induced caster breakouts.

Production route	Al-killed steel	Si-killed steel
Non-degassing	occasional	occasional
Degassing	very few	occasional

When casting non-degassed Al-killed steels, which have a rather high hydrogen content, hydrogen-induced breakouts occasionally occur. It is well known that the frequency of such breakouts strongly depends on the hydrogen content and casting speed, and particularly careful operation is required if the hydrogen content exceeds 8 ppm[1]. It was clearly measured during laboratory-scale chill-block experiments that the pressure of the gaseous hydrogen emitted from the solidified shell topped 1 atm at the early stage of solidification when the hydrogen content in the molten steel exceeded 7 ppm[2,3]. As excessive gas suspended as bubbles in the flux films strongly inhibit heat extraction[4], hydrogen pickup which comes from moisture in the many kinds of additions in steelmaking and casting operations, should be minimized[5,6]. Based on practical operations, a breakout warning system combined with precise hydrogen analysis was also reported to minimize the possibility of breakouts[7]. Practical knowledge has already been reported as mentioned above, however, it seems that there is still insufficient understanding about the basic kinetics of hydrogen gas evolution behavior under actual casting conditions. In order to better our understanding, we analyzed hydrogen diffusion and chemical reactions between the solidified shell and gas pores at several plant operations.

New knowledge was added to prevent breakouts of Si-killed degassed steels by one of the present authors[8]. Although these steel grades have low enough hydrogen content, caster breakouts still occurred occasionally. Chemical reactions between the ambient atmosphere, mold flux and molten steel was focused on with the help of NMR analysis of the mold flux, whereupon it was concluded that hydroxyl (OH^-) ions were initially absorbed from the ambient water vapor into the molten layer of the mold flux during casting, and then accumulated because of the weak reducing power of Si-killed steels, and finally, due to decomposition of the hydroxyl ions in mold flux film cooled by the low-temperature mold surface, bubbles of water vapor evolved and resulted in breakouts. On the basis of these analyses, effective ways to prevent breakouts were found.

2. Hydrogen-induced breakouts in Al-killed non-degassed steels [9]

2.1 Analysis of mold flux after casting

Casting results for two non-degassed Al-killed steels with different hydrogen contents are shown in Table 2 and Fig. 1. The photographs are of mold fluxes for Case I after stable casting and Case II after caster breakout. These were the results from a vertical-bending type 250-mm-thickness slab caster. Casting speeds were 1.3 m/min, basicity (CaO/SiO_2) of the mold fluxes was 1.3, and steel compositions were 0.08%C-0.3%Si-1.3%Mn in both cases. In Case I, the strand-facing surface of the mold flux was quite smooth, and few pores were found at the cross section. On the other hand, in Case II, there were many pores on the strand-facing surface of the mold flux and at the cross section. From the result of gas analysis of the mold flux, gaseous species in these pores were mainly identified as H_2 and H_2O.

Table 2 Casting conditions and results.

Case	H in mold (ppm)	Q ($Gcal/m^2/hr$)	Result
I	6	1.23	Stable operation
II	11	0.94	Caster breakout

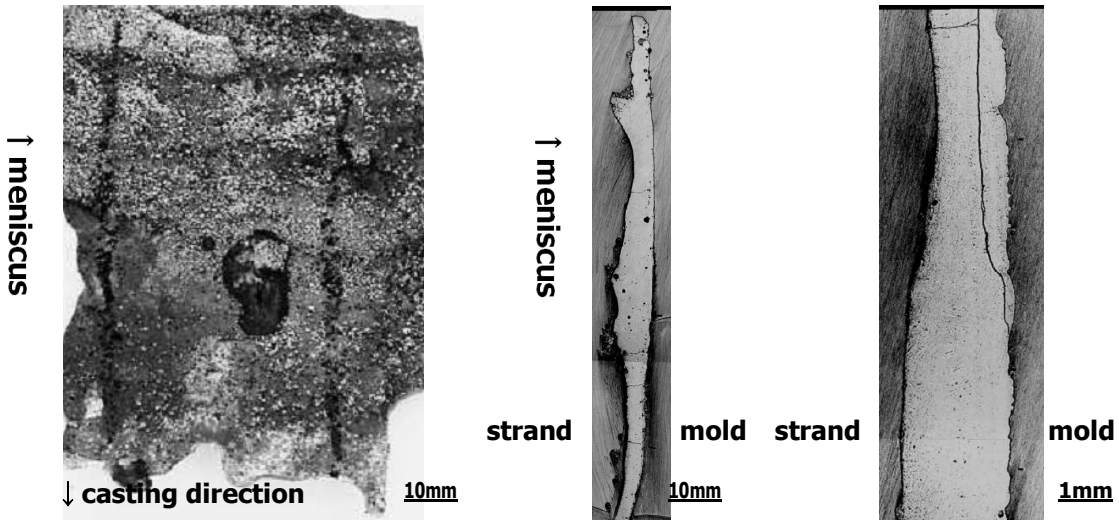

(a) external view facing strand (b) cross-sectional views

Case I Non-degassed Al-killed steel containing 6 ppmH.

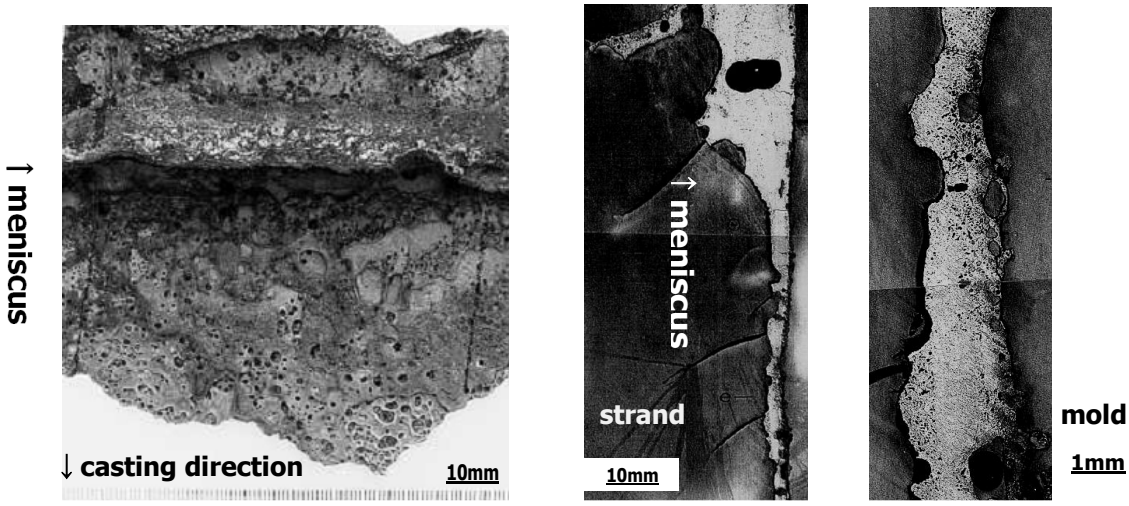

(a) external view facing strand (b) cross-sectional views

Case II Non-degassed Al-killed steel containing 11 ppmH.

Fig. 1 Mold flux around meniscus in molds after casting. No pores were found in Case I, whereas many existed in Case II [9].

2.2 Hydrogen diffusion from solidified shell to molten flux film and gas evolution at mold meniscus

Evolution of hydrogen gas at the mold meniscus is schematically shown in Fig. 2. The evolution rate was calculated with Eqs.(1)〜(5), where three assumptions were taken into consideration: (i) one-dimensional heat transfer, (ii) one-dimensional diffusion of supersaturated dissolved hydrogen in the solidified shell, which is the rate-determining step of the evolution of hydrogen gas, and (iii) local equilibrium of hydrogen between the solidified shell and gas pores. The meanings of the symbols and physical properties necessary for these calculations are shown in Table 3 and Fig. 3.

$$C \cdot \rho \cdot \partial T/\partial t = k \cdot \partial^2 T/\partial x^2 + L \cdot \rho \cdot \partial fs/\partial t \quad (1)$$

$$Q = h \cdot (Ts - To) \qquad \text{at } x = 0 \quad (2)$$

$$\partial [H]/\partial t = D \cdot \partial^2 [H]/\partial x^2 \quad (3)$$

$$K = [H]/\sqrt{P_{H2}} \qquad \text{at } x = 0 \quad (4)$$

$$J = -D \cdot \rho/(100 \cdot W_{H2}) \cdot \partial [H]/\partial x \qquad \text{at } x = 0 \quad (5)$$

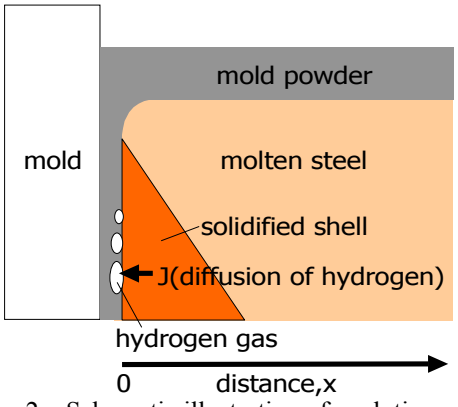

Fig. 2 Schematic illustration of evolution of hydrogen gas bubbles beneath mold meniscus.

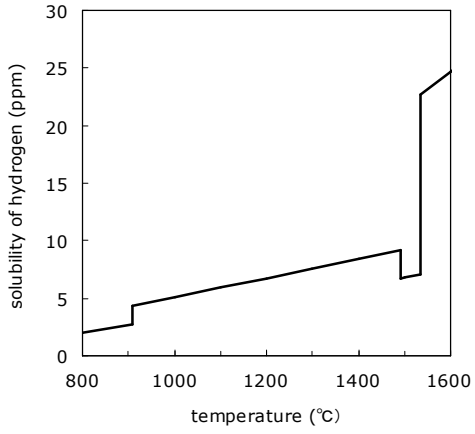

Fig. 3 Solubility of hydrogen in pure iron [10].

Table 3 Symbols and physical properties[10,11].

Symbol	Quantity	Unit	Value
C	specific heat capacity of steel	cal/g/K	0.18
D(δ)	diffusion coefficient of hydrogen in δ phase	cm^2/s	0.0101exp(-11293/RT)
D(γ)	diffusion coefficient of hydrogen in γ phase	cm^2/s	0.00109exp(-2297/RT)
[H]	hydrogen content in solidified shell	wt%	
J	hydrogen flux	$mol/cm^2/s$	
K(δ)	equilibrium constant of $1/2H_2(g)=[H]$ in δ phase	-	$10^{(-1418/T-2.369)}$
K(γ)	equilibrium constant of $1/2H_2(g)=[H]$ in γ phase	-	$10^{(-1182/T-2.369)}$
L	latent heat of solidification of steel	cal/g	65
P_{H2}	partial pressure of hydrogen gas	atm	
Q	heat flux	$cal/cm^2/s$	
T	absolute temperature	K	
Ts	surface temperature	K	
To	temperature of cooling water in mold	K	
W_{H2}	molar weight of hydrogen gas	g/mol	
fs	fraction of solid phase of steel	-	
h	heat transfer coefficient	$cal/cm^2/s/K$	1000
k	thermal conductivity of steel	cal/cm/s/K	0.08
t	time after start of solidification	s	
x	depth from surface of solidified shell	cm	
ρ	density of steel	g/cm^3	7.3

Calculated results are shown in Fig. 4. In casting steel containing 6 ppmH(Case I), gaseous hydrogen does not evolve, and nor does hydrogen diffuse into the solidified shell. On the other hand, in casting steel containing 11 ppmH(Case II), gaseous hydrogen begins to evolve immediately after solidification starts, and the thickness of the hydrogen gas film one second after solidification, when the corresponding depth is 20 mm beneath the mold meniscus, exceeds the average powder film thickness evaluated from the powder consumption rate under this casting condition. It was found that such rapid hydrogen evolution immediately after the start of solidification would strongly inhibit heat extraction, resulting in caster breakout. Consequently, lower dissolved hydrogen content and higher mold powder consumption rates are preferable to prevent hydrogen-induced breakouts.

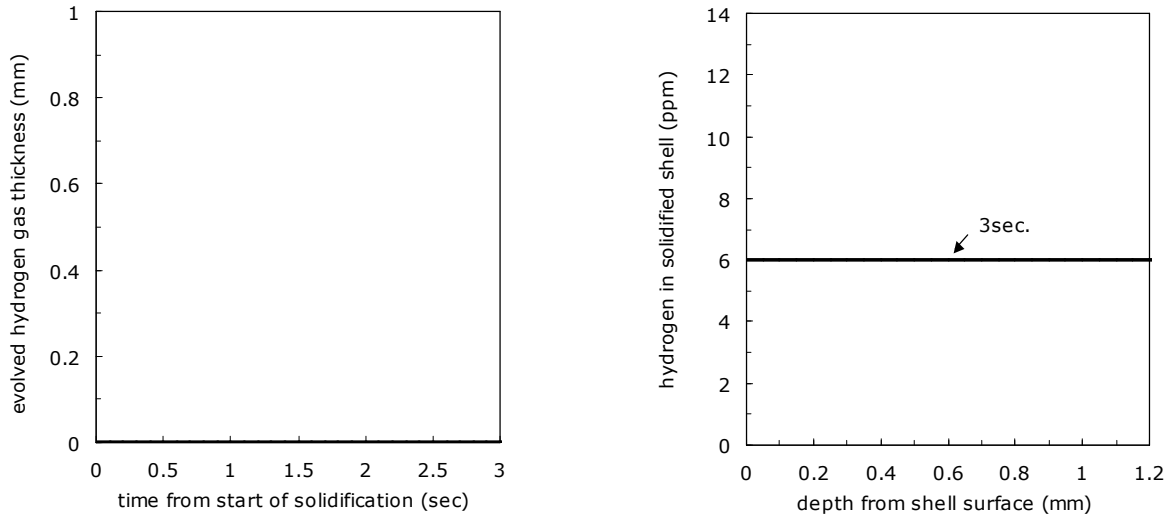

Case I Non-degassed Al-killed steel containing 6 ppmH.

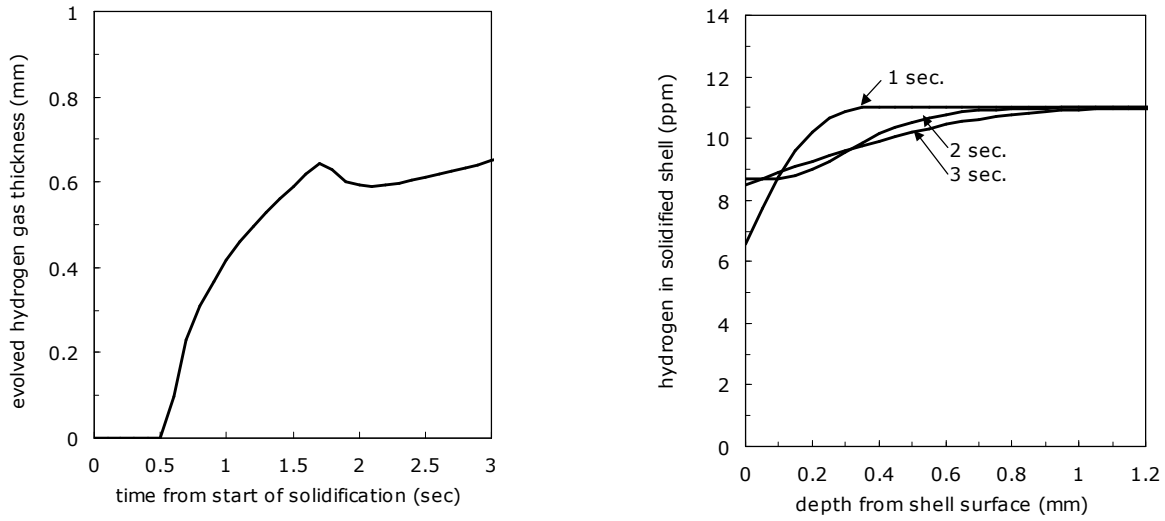

Case II Non-degassed Al-killed steel containing 11 ppmH.

Fig. 4 Calculated values of hydrogen evolved from solidified shell (left) and dissolved hydrogen in solidified shell beneath mold meniscus several seconds after start of solidification (right). No hydrogen evolves in Case I, whereas it begins immediately after solidification starts in Case II. There is good agreement between observations and calculations in both cases [9].

3. Hydrogen-induced breakouts in Si-killed degassed steels [8]

3.1 Analysis of mold flux after casting

Hydrogen-induced breakouts occasionally occur in Si-killed degassed steels. As they rarely occur in Al-killed degassed steels, these two kinds of steel grades were compared, that is, one was an Al-killed degassed steel (Case III) and the other was a Si-killed degassed steel (Case IV). Steel compositions were 0.08%C-0.01%Si-0.4% Mn-0.03%Al for the Al-killed steel and 0.08%C-0.08%Si-0.4%Mn-0.005%Al for the Si-killed steel, respectively. In both cases, the hydrogen content of the steel was 4 ppm in the tundish, casting speeds were 1.6 m/min, and the basicity (CaO/SiO_2) of the mold powders was 1.1.

Cross-sectional structures of the mold fluxes after casting are shown in Fig. 5. There were no pores in the mold flux in Case III after stable casting of the Al-killed steel, whereas many pores were observed inside the flux in Case IV after casting the Si-killed steel. From gas analyses, water vapor (H_2O) was mainly detected as the gaseous species in the gas pores.

Dissolved OH^- ion concentrations in the mold flux were also measured using NMR, as shown in Fig. 6. The OH^- ion concentration decreased during casting in Case III of the Al-killed steel, whereas it evidently increased from 80 ppm to 140 ppm in Case IV of the Si-killed steel.

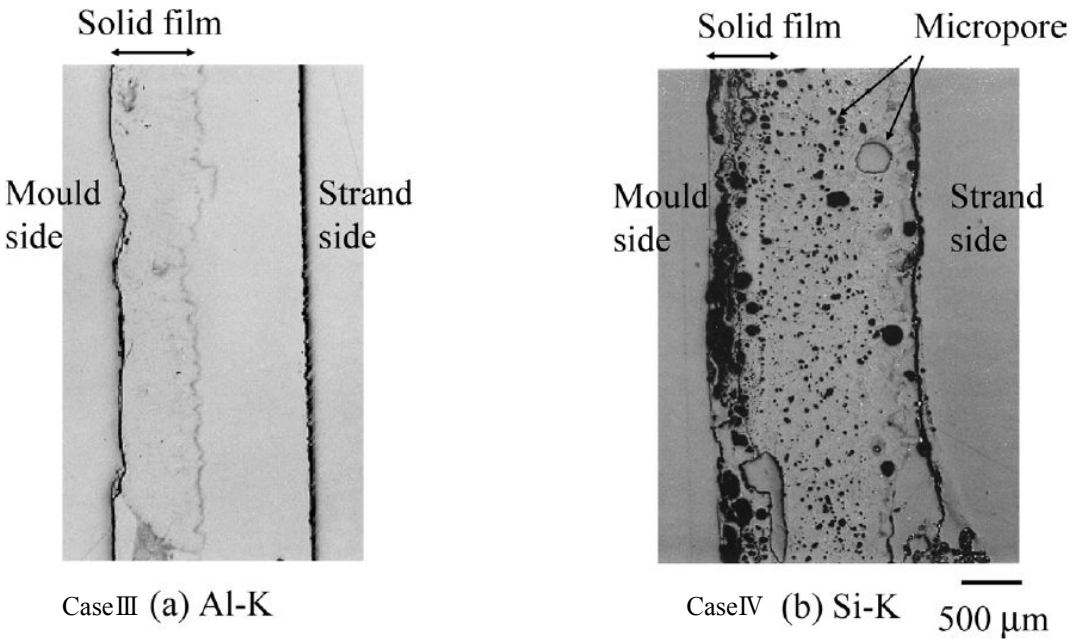

Fig. 5 Cross-sections of molten flux films beneath mold meniscus. No pores were found in Case III ((a) Al-killed degassed steel), whereas many gas bubbles existed in Case IV ((b) Si-killed degassed steel) [8].

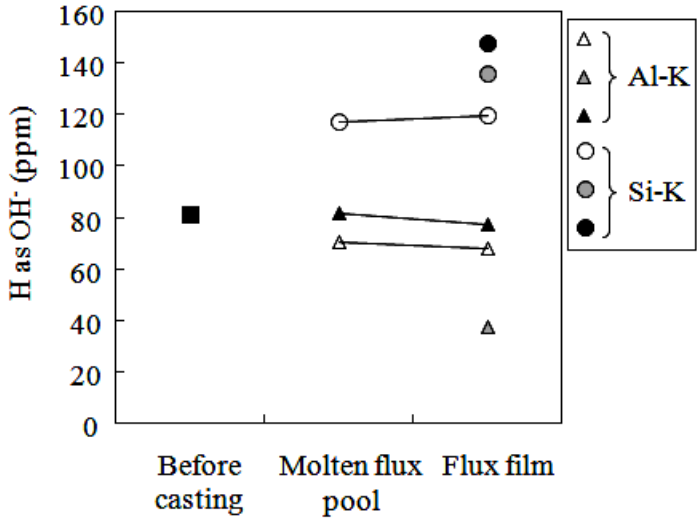

Fig. 6 Change in OH-ion contents in mold flux during casting, as determined by NMR analysis. OH-ions slightly decomposed during casting in Case III (Al-killed degassed steel), whereas they accumulated significantly in Case IV (Si-killed degassed steel) [8].

3.2 Evolution of water vapor inside mold flux at mold meniscus

Based on the analysis mentioned above, evolution behavior of water vapor bubbles was estimated as shown in Fig. 7 and Eqs.(6)~(9). Initially, moisture in the ambient atmosphere dissolves into the mold flux as hydroxide ions during casting. As the hydroxide ions are sufficiently reduced by the strong reduction power of the dissolved Al in Case III(Eq. (7)), no accumulation of hydroxide ions occurs in the mold flux of the Al-killed degassed steel. Conversely, as OH^- ions are not sufficiently reduced (Eq.(8)) due to the weak reduction power of the Si-killed steel in Case IV, a significant volume of OH^- ions surely accumulates. When the mold flux infiltrates the channel between the low-temperature mold

surface and the solidified shell, it should become supersaturated with OH^- ions, and then immediately water vapor evolves by decomposition of supersaturated OH^- ions (Eq.(9)). We considered that this was the main reason for the occasional breakouts affecting Si-killed degassed steel, and thus a lower SiO_2 concentration of mold flux should be preferable to promote reduction of the OH^- ions (Eq.(8)). Based on this concept, a new mold powder was designed whose basicity (CaO/SiO_2) was raised to 1.8. Caster breakouts were successfully prevented by applying the new mold powder to actual casting operations, and no accumulations of OH^- ions with very few pores inside the molten flux infiltrating into the mold channel were also confirmed, as shown in Figs. 8 and 9.

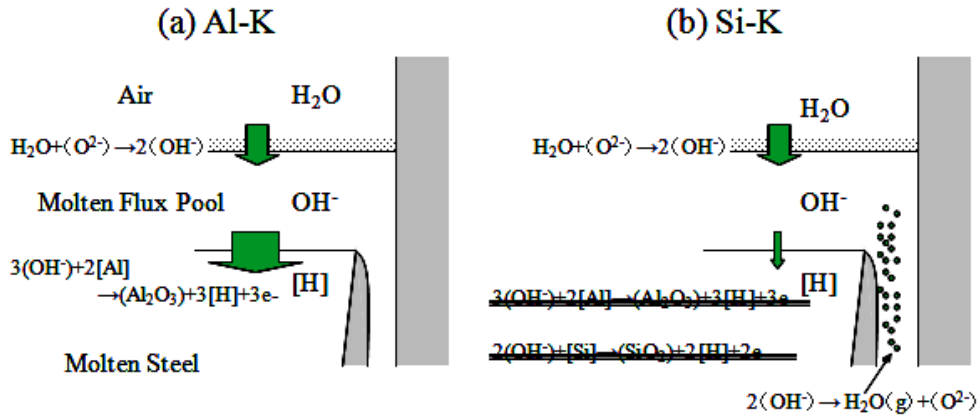

Fig. 7 Evolution of H_2O gas bubbles in mold flux during casting of degassed Si-killed steel (right) [8].

$$H_2O(g)+(O^{2-})=2(OH^-) \quad (6)$$

$$6(OH^-)+2[Al]=(Al_2O_3)+6[H]+3(O^{2-}) \quad (7)$$

$$4(OH^-)+[Si]=(SiO_2)+4[H]+2(O^{2-}) \quad (8)$$

$$2(OH^-)=H_2O(g)+(O^{2-}) \quad (9)$$

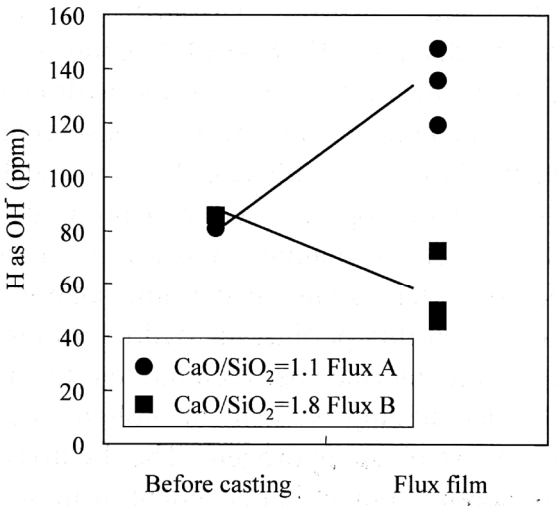

Fig. 8 Change in concentration of OH^- ions during casting. OH^- ions did not accumulate upon applying the improved flux (Flux B) [8].

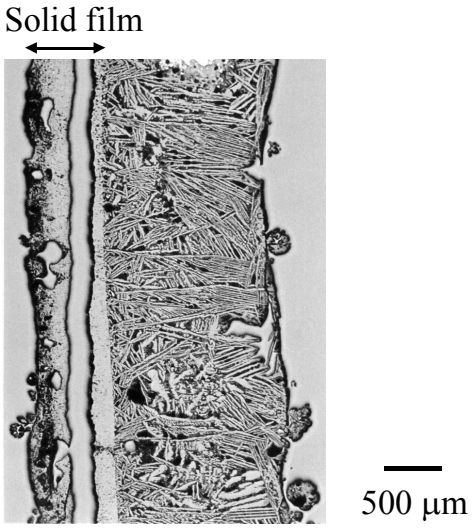

Fig. 9 Cross-section of improved mold flux. Water vapor pores were successfully minimized [8].

4. Conclusion

Two kinds of hydrogen-induced caster breakouts were analyzed. It is concluded that less dissolved hydrogen content and higher consumption rates for mold powder in the case of Al-killed non-degassed steels, and a higher basicity of mold powder for Si-killed degassed steels are surely preferable to prevent hydrogen-induced breakouts.

References

[1] P. Zasowski, D.J. Sosinski. Control of heat removal in the continuous casting mould. *Steelmaking Conf. Proc.*, 1990, p.253-259.

[2] H. Mizukami, T. Shirai, T. Watanabe. Evolution of hydrogen gas from molten steel at initial stage of solidification. *CAMP-ISIJ*, 2003,16, p.951.

[3] H. Mizukami, M. Hara, T. Shirai, T. Watanabe. Generation of hydrogen gas from solidified shell surface at initial stage of solidification of carbon steel. *ISIJ Int.*, 2004, 44, p.1714-1719.

[4] H. Kyoden, T. Doihara, O. Nomura. Development of mold powders for high speed continuous casting of steel. *Steelmaking Conf. Proc.,* 1986, p.153-159.

[5] J.H. Park, J.S. Park, J.Y. Ko. Improvement of slab surface quality by the use of sintered and fused mould fluxes. *Steel Times*, 1998, 9,p.CC14-CC15.

[6] S. Misra, Y. Li, I. Sohn. Hydrogen and nitrogen control in steelmaking at U.S.Steel. *Iron Steel Tech.,*2009, 11, p.43-52.

[7] S. Abraham, S. Chen, J. Asante, C. D'Souza. Hydrogen and nitrogen control and breakout warning model for casting non-degassed steel. *Iron Steel Tech.,* 2010, 10, p.54-64.

[8] T. Kajitani, Y. Kato, K. Harada, K. Saito, K. Mizukami, W. Yamada. Mechanism of a hydrogen-induced sticker breakout in continuous casting of steel: Influence of hydroxyl ions in mould flux on heat transfer and lubrication in the continuous casting mould. *ISIJ Int.,* 2009, 48, p.1215-1224.

[9] Y. Ueshima, T. Mizoguchi, Y. Takagi, K. Kondo, H. Kato. *ISIJ Int.,* to be submitted.

[10] H.Bester, K.W. Lange. Abschätzung mittlerer Werte für die Diffusion von Kohlenstoff, Sauerstoff, Wasserstoff, Stickstoff und Schwefel in festem und flüssigem Eisen. *Arch.Eisenhüttenw.,* 1972, 43, p.207-213.

[11] Ed.by the 19th committee on steelmaking, The Japan Society for Promotion of Science. Recommended Values of Chemical Equilibrium for Steelmaking, in Japanese, 1984, p.8.